

EXPERIMENTAL INVESTIGATION OF FLOW THROUGH A PRESSURE SWIRL ATOMIZER AND THE RESULTING HOLLOW CONE SPRAY AT DIFFERENT OPERATING CONDITIONS

Bülent SÜMER¹
TÜBİTAK-SAGE
Ankara, Turkey

Nejdet ERKAN²
University of Tokyo
Tokyo, Japan

Oğuz UZOL³
and
İsmail H. TUNCER³
Middle East Technical University
Ankara, Turkey

ABSTRACT

In the present study the flow through a pressure swirl atomizer and the properties of the resulting hollow cone spray are investigated using experimental techniques for different operating conditions. High-speed direct shadowgraph system is used to visualize the aircore inside the pressure swirl atomizer and the resulting hollow cone spray. Two high-speed cameras are used in sync mode for the visualization. The images captured are analyzed quantitatively with a developed image processing tool, to obtain the aircore diameter. The microscopic properties of the spray are investigated using a two-component Phase Doppler Particle Analyzer. The droplet size and velocity distributions are obtained at different spatial locations. The liquid flow structure is investigated by analyzing the properties of different droplet size classes.

INTRODUCTION

Pressure swirl atomizers are widely used in combustion systems utilizing liquid fuels. In the case of liquid rocket engines (LRE), pressure swirl atomizers can be used as fuel and oxidizer atomizers, together forming a bipropellant liquid rocket injector. Pressure swirl atomizers convert the potential energy in the form of pressure drop to kinetic energy of the propellants and atomize and mix them. As the pressure drop across the atomizer increases, more mass of propellant flows through the atomizer. In the case of LRE the mass flow rate of propellant through an atomizer is known a priori from a LRE performance analysis. For a fixed flow rate of propellant the aim is to efficiently atomize and mix propellants with minimum energy.

In pressure swirl atomizers the propellant is fed through the tangential inlet passages into the swirl chamber. A liquid vortex with a free surface is formed within the atomizer. The radius of the free surface changes from minimum at the base of the swirl chamber to a larger value at the exit of the nozzle. A thinner liquid film exits through the nozzle and eventually breaks up into fine droplets forming a hollow cone spray (Figure 1).

¹ Chief Research Engineer, Email: bulent.sumer@tubitak.gov.tr

² Assistant Professor, Email: erkan@vis.t.u-tokyo.ac.jp

³ Professor, Email: tuncer@ae.metu.edu.tr, uzol@metu.edu.tr

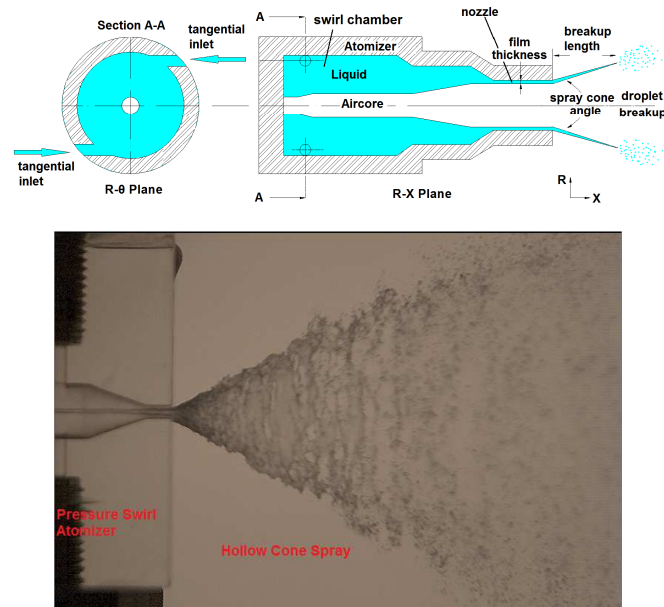


Figure 1: Pressure swirl atomizer and the hollow cone spray.

Despite the geometric simplicity of the pressure swirl atomizer, the hydrodynamic processes occurring within the nozzle are highly complex. The formation of aircore within the atomizer makes the flow inside the atomizer a free surface flow. It is possible to perform an initial sizing study for a pressure swirl atomizer using analytical methods [Abramovich1944], [Bavyel1993], [Giffen1953] at a design point with some level of fidelity, but it is not possible to deduce the off-design performance of the atomizer with analytical equations.

In this paper, flows inside a pressure swirl atomizer, whose characteristics were studied previously by Sumer et. al. [Sumer2012] using numerical and experimental methods are investigated experimentally for different operating conditions. In addition microscopic spray properties of the resulting hollow cone spray are characterized.

METHOD

Both numerical and experimental methods can be used to study the off-design performance of pressure swirl atomizers. The unsteady numerical simulations give satisfactory results, but they are expensive to perform due to the two-phase nature of the problem. On the other hand, experimental methods, which are mainly focused on measuring the aircore diameter or the liquid film thickness, are easier to implement. In order to measure the aircore diameter or the liquid film thickness, the electrical conductance method [Suyari1986, Kim2009, Fu2011] and the photographic method [Som1980, Som1983, Som1984, Dash2001, Moon2010] are mostly used in previous studies. The electrical conductance method uses a pair of probes in order to locally measure the conductance which is a function of the thickness of the film between the probes. In theory it is possible to take measurement at each location of interest as long as the necessary probes are installed on the test item, but in practical applications only one probe can be used at location of interest [Fu2011]. If an optical access is available, photographic techniques can be used to visualize the aircore and it is possible to study the major characteristics of the flow at any location by processing the obtained images [Moon2010]. In the present study high speed shadowgraphy technique is used to visualize the flow inside a Plexiglas atomizer.

The most efficient method that is used for spray characterization is the phase Doppler anemometry method. Phase Doppler anemometry (PDA) is a non-intrusive technique for the sizing of spherical particles (typically liquid sprays, but also some bubbles and solid spheres). The phase Doppler anemometry technique is an extension of the laser Doppler anemometry technique (LDA). In PDA along with the velocity of the particle, the size of the particle is also obtained. The phase Doppler

principle was first reported by Durst [Durst1975], who showed that the method can be applied to velocity measurements of reflecting and refracting particles. Later Bachalo [Bachalo1984] used the phase Doppler principle to develop a viable technique for drop size and velocity measurements.

Cold Flow Test Facility

The cold flow test facility consists of a 40 liters water tank which can stand pressures up to 200 bars. An industrial type nitrogen cylinder, which is equipped with a pressure regulator, is used to pressurize the water tank to drive the water from tank to atomizer. A needle valve controls the flow rate of water to the atomizer. Turbine type flow meters are used for the measurement of water flow rate. Main line from the water tank branches into two after the flow meter and water is fed into the atomizer from two tangential inlet passages. Both branches are equipped with pressure transducer to check whether the flow rates are identical.

Pressure Swirl Atomizer

The internal geometry of the pressure swirl atomizer studied is given in Figure 2a. The total length of the atomizer was 17.5 mm and the length of the nozzle was 4 mm. The diameter of the swirl chamber and the nozzle of the atomizer were 8 mm and 2 mm, respectively. Water is fed through two tangential inlet passages; whose diameter is 2.54 mm. Pressure swirl atomizer is manufactured from Plexiglas in order to visualize the aircore inside the atomizer at high temporal and spatial resolutions (Figure 2b).

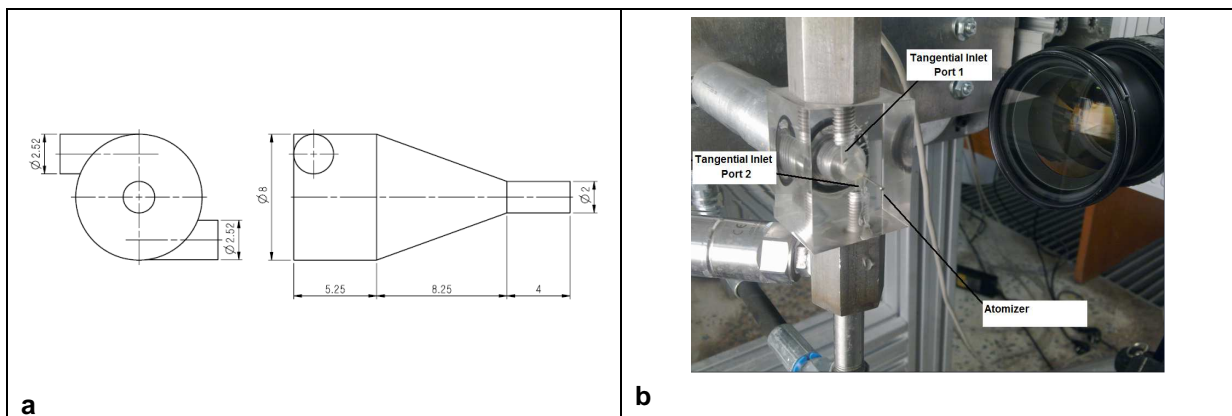


Figure 2a: Geometrical dimensions of the pressure swirl atomizer (all dimensions are in millimeters) b: Plexiglas pressure swirl atomizer on cold flow test facility.

High Speed Shadowgraphy System

High-speed direct shadowgraph system is used to visualize the aircore inside the pressure swirl atomizer and the resulting hollow cone spray. Two high-speed cameras are used in sync mode for the visualization. One camera (Camera2) equipped with a 60 mm 1:2.8 D macro lens records the flow inside the pressure swirl atomizer and the other one (Camera1) equipped with a 24-85 mm 1:2.8-4d lens records the resulting hollow cone spray. The backlight illumination of the atomizer is achieved by using a light emitting diode (LED) whose light intensity can be adjusted. A set of collimating optics (a condenser lens and a Fresnel lens) delivered the green light from LED to the atomizer. The backlight illumination of the spray is obtained with a halogen lamp and a diffuser screen. Light sources and the cameras are aligned at the opposite sides as shown in Figure 2a. The effective image areas for Camera1 and Camera2 are 576x464 pixels (115x92mm) and 768x368 pixels (28x13mm), respectively. The frame rate for both cameras is 20 kHz. The images taken are processed with an image processing tool developed in-house.

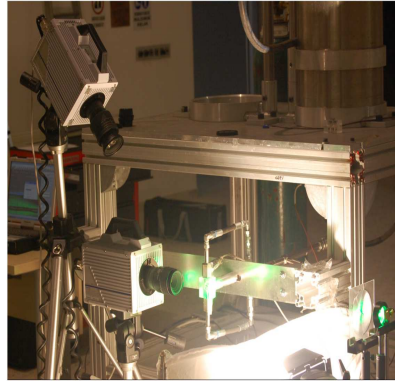


Figure 3: High speed shadowgraphy setup on cold flow test facility.

Image Capturing and Processing

The resolution for both high speed CMOS cameras is a function of the frame rate at which the images are collected. Cameras have a resolution of 1024x1024 pixels at 5400 frame per second (fps) and they can go up to 675000 fps for a resolution of 64x16 pixels. After adjusting the frame rate and supplying the sufficient illumination, the high speed shadowgraphy system is ready to capture movies. The captured movies were stored at camera memory and then they were saved to the computer as movie files. The movie files were then converted to image files using Photron Fastcam Viewer.

The captured images of the aircore inside a pressure swirl atomizer and the resulting spray at one instant of time are shown in Figure 4 for illustration. Water is flowing through the atomizer and forming a hollow cone spray as shown.

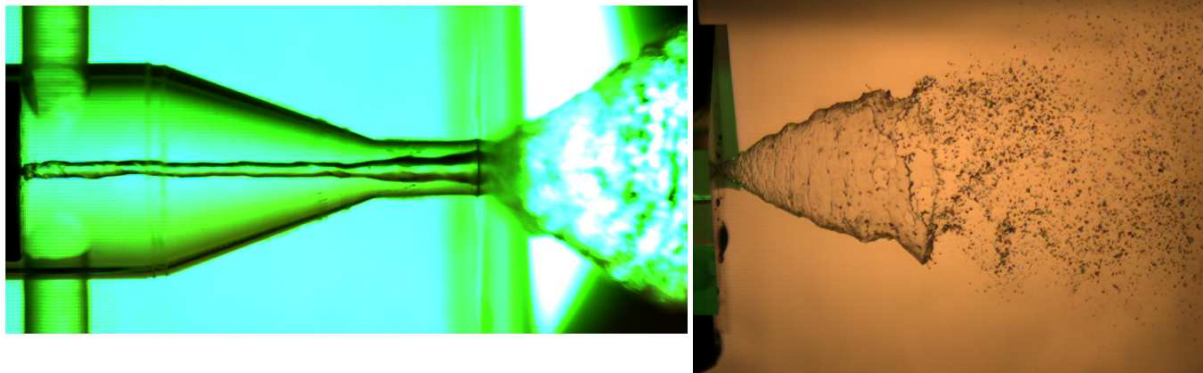


Figure 4: Images of the aircore inside the atomizer (left) and the resulting hollow cone spray (right).

The sample images (Figure 4) which are showing the aircore inside the atomizer and the hollow cone spray has one distinct property. The edges of the interfaces are easily discerned due to high density gradients, and show themselves as darker regions at aircore and spray boundaries. The diameter of the aircore at any location within the atomizer can be obtained by detecting the edges and measuring the distance between two edges. Similarly the distance between spray boundaries can be found at any downstream location from the atomizer exit and the spray cone angle can be determined.

Edge detection is a low level operation used in image processing and computer vision applications. The main goal of edge detection is to locate and identify sharp discontinuities from an image. These discontinuities are due to abrupt changes in pixel intensity which characterizes boundaries of objects in an image. Edges give boundaries between different regions in the image [Bhardwaj2012]. These object boundaries are the first step in many of computer vision algorithms like edge based face recognition, edge based obstacle detection, edge based target recognition, image compression etc. So the edge detectors are required for extracting the edges.

In order to use the edge detection operators efficiently, the RGB images obtained using the high speed cameras were first converted to grayscale images. A sample RGB image and the grayscale image are shown together in Figure 5.

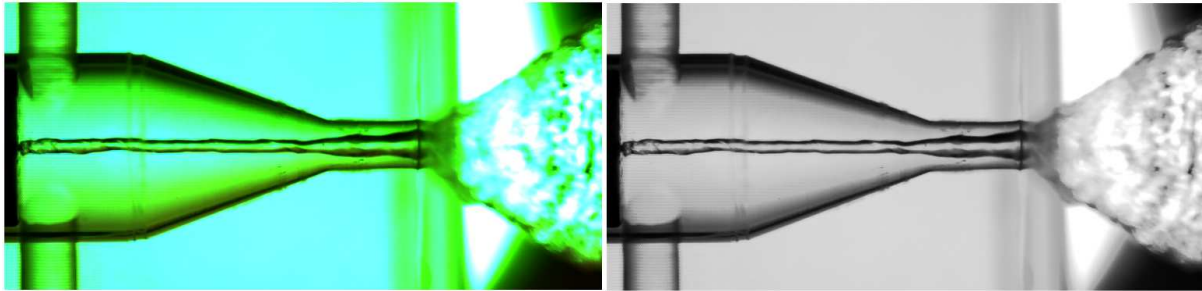


Figure 5: Conversion of RGB image to grayscale image.

After the conversion an appropriate edge detector was applied to the grayscale image in order to find the edges. Among the various edge detectors, Sobel edge detector was found to be the most effective edge detector for the captured images. Mathematically, the Sobel operator uses two 3x3 kernels which are convolved with the original image to calculate approximations of the derivatives; one for horizontal changes, and one for vertical changes.

An image processing program was developed in MATLAB to process the obtained images. The image processing consists of converting the RGB image to grayscale image, subtracting the background image and increasing the intensity, if necessary, and finding the edges using Sobel edge detector as shown in Figure 6. The image that is shown in Figure 6 can then be used to find the aircore diameter at any axial location within the atomizer.

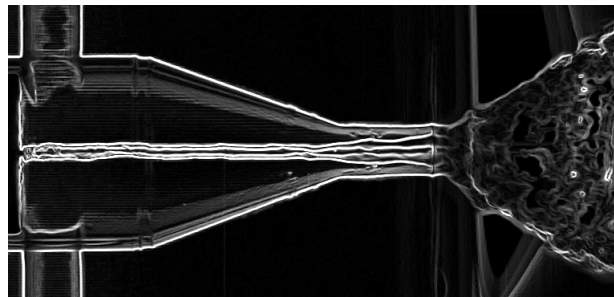


Figure 6: The sample image after application of Sobel edge detector.

Phase Doppler Particle Analyzer System

In PDA technique, interference patterns are produced at the crossing volume of two laser beams (measurement volume or probe volume). The interference patterns are a series of light and dark fringes. As the particle moves through the measurement volume, it scatters light as it crosses a bright fringe, and scatters no light as it crosses a dark fringe. This results in a fluctuating pattern of scattered light intensity with a frequency proportional to the particle velocity. This frequency is known as the Doppler shift frequency, which is identical in all spatial directions. In addition to its capability of measuring particle velocities, the PDA technique can also determine the diameter of particles. When viewed from two separate spatial locations the scattered signals exhibit a phase shift whose magnitude depends on factors including the angle at which light is scattered to each photodetector, the index of refraction of the material of the spherical particle, and parameters such as the light wavelength and the beam intersection angle. The phase shift measured in the Doppler signal obtained from the same particle using two closely spaced photodetectors varies linearly with the particle diameter. The PDA technique makes use of the phase shift measured in Doppler signal to determine the diameter of the particles.

A schematic of the phase Doppler anemometry system, showing the major components, is given in Figure 7.

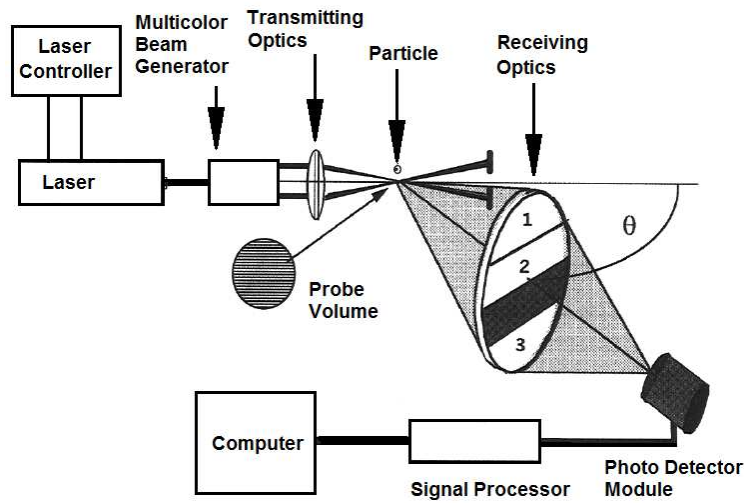


Figure 7: Schematic of phase Doppler anemometry system.

The PDA system transmitter package consists of a laser, a multicolor beam generator and a transmitter. In the most general case of three components PDA, the multicolor beam generator separates the beam coming from the laser into green, blue and violet beams and split each beam into two beams of preferably same power. The beams are carried to the transmitter optics by using fiber optic cables and they go into the transmitting optics as two parallel beams. Then the parallel beams are deflected by the transmitting optics and caused to intersect at a point. The beam crossover volume is called the probe volume.

The receiver package of the PDA system consists of receiver optics which collects the light scattered by droplets within the probe volume and focused it onto a pinhole. Light which passed to pinhole was directed by mirrors to photo detectors. The mirrors are adjusted so that the light from different well-defined areas of the receiver lens is directed to individual photo detectors through fiber optic cables. The photo detector module contains the photo detectors, which are extremely sensitive detectors of light in the ultraviolet, visible, and near-infrared ranges of the electromagnetic spectrum. Photo detectors generate electrical signals which represent incoming optical signals. The signal processor receives and processes analog burst signals from the photo detectors and sends the results to computer.

Phase Doppler Particle Analyzer

A two-component phase Doppler particle analyzer (PDPA; TSI Inc.) was used to study the microscopic properties of the hollow cone spray developed by the pressure swirl atomizer. The transmitter optics and the receiver optics were positioned on a three-axis remote-controlled traverse system as shown in Figure 8.

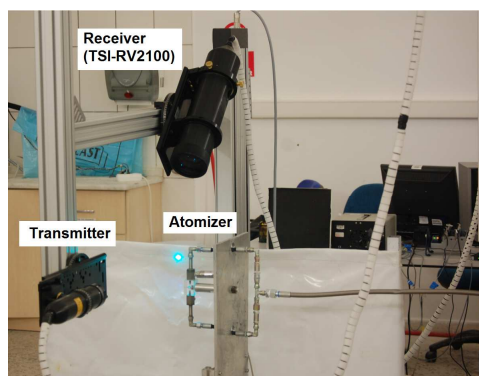


Figure 8: Transmitter and receiver optics positioned on three-axis traverse.

The transmitter package of the PDPA has an Ar-Ion laser (Coherent Innova 70-5) which has a maximum power output of 5 Watts at multiline blue/green. The multiline laser beam goes into the multicolor beam generator (Fiberlight). The Fiberlight takes the multiline laser beam and separate it to green ($\lambda=514.5$ nm) and blue ($\lambda=488$ nm) beams. Both blue and green laser beams are further splitted into two laser beams (shifted and unshifted beams) by a set of optics that are positioned within the Fiberlight. The shifted and unshifted beams are transmitted from Fiberlight to the fiberoptic cables by using Aerometrics type couplers. These couplers contain the necessary optics to focus the laser beam to the tips of the fiberoptic cables. The beams are transferred to the fiberoptic transmitting probe through fiberoptic cables. The fiberoptic transmitter probe contains the necessary optical elements to collimate the beams from the fiberoptic cables (collimating lenses), expand them as needed (beam expander) and deflect the beams such that they intersect to form the probe volume (focusing lens).. The focal length of the focusing lens used in the present study is 500 mm and the calculated values for the beam waist diameter and fringe spacing are 185 μm and 12.8 μm , respectively. The minimum and maximum droplet diameters that can be measured with the optical setup are about 1.23 μm and 514.55 μm , respectively.

As a spherical particle passes through the probe volume it scatters light in all directions. The receiver package of the PDPA consist all necessary optical and electronic elements to collect the scattered light, convert them to electrical signals and extract information from these signals. The light scattered by the particle is collected by a receiver (Figure 8). The receiver has a lens assembly which collects the light scattered by droplets and focused it onto a multimode fiber. The multimode fiber transmits the light to the photodetectors. The photodetectors, which are contained in the photo detector module (PDM), converts the light transmitted by the multimode fibers into electrical signals (voltage). The photodetectors that are used in the present study are photomultiplier tubes (PMT) which are extremely sensitive detectors of light. The PDM sends the electrical signals to the FSA signal processor. The FSA signal processor receives these signals and extracts information such as frequency, phase, burst transit time and burst arrival time from these signals and sends it to a computer. The receiver that was used in the present study had a front lens with a focal length of 500 and a back lens with a focal length of 370 mm. The slit used in the present study had an aperture of 150 μm .

The receiver and transmitter are positioned on a 3-axis traverse in a 43° forward scatter configuration.

RESULTS AND DISCUSSION

Formation of the Aircore and the Spray

The high speed shadowgraphy setup was used to visualize the formation of the aircore within the atomizer and the hollow cone spray. Initially the atomizer was filled with water. The needle valve was opened from closed position to open position, while the high speed cameras were recording. The aircore formation within the atomizer and spray formation are shown with nine images in Figure 9. Each image shows the atomizer on the left and spray on the right. The sampling period of the images shown in Figure 9 was 7.5 milliseconds (ms.) and a fully developed spray was formed at about 60 ms.

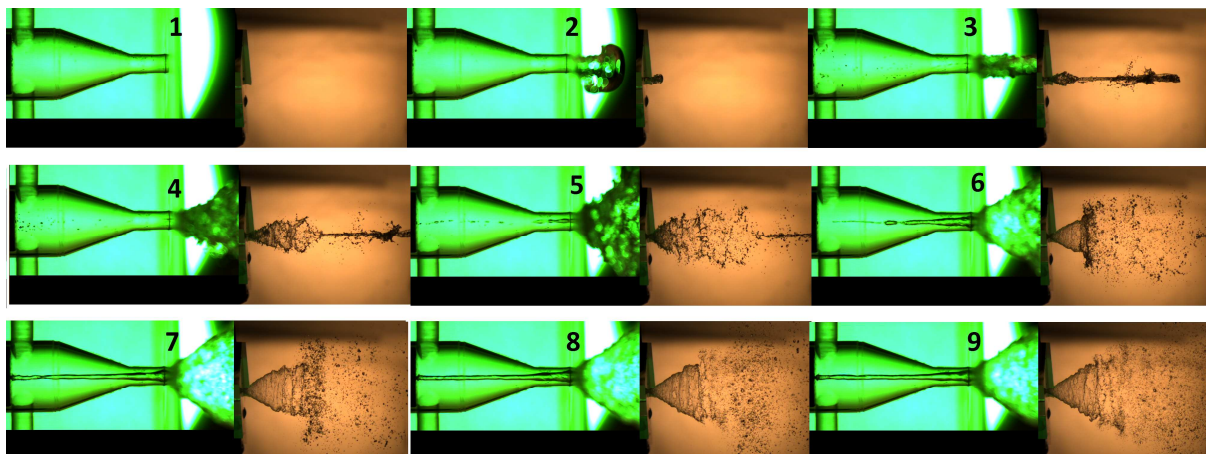


Figure 9: Formation of the aircore and the hollow cone spray.

The formation of the aircore with in the atomizer started with the depletion of the water at the nozzle of the atomizer (image 4) and the formation of the full aircore took about 20 ms. On the other hand some stages of the spray development can also be identified by looking at Figure 9. At low flow rates the spray was like a distorted pencil (image 3) and as the flow rate increases the spray evolved to an onion (image4) and then to a tulip shape (image 9).

Aircore and Spray at Different Operating Conditions

In order to investigate the performance of the atomizer at different operating points the mass flow rate through the atomizer was increased by adjusting the needle valve. The flow rate through the atomizer is plotted against the pressure drop across the atomizer in Figure 10.

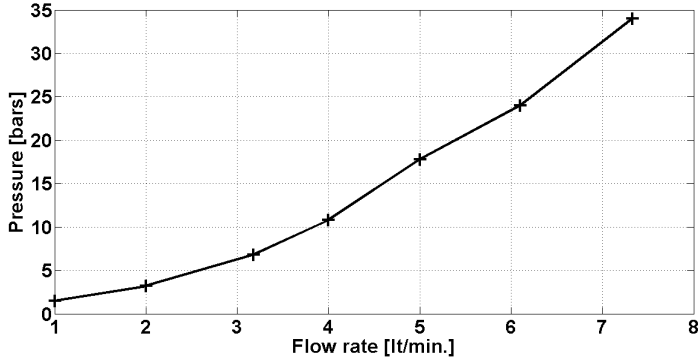


Figure 10: Flow rate versus pressure drop graph.

As discussed in the previous section the formation of the aircore was rapid and occurred at a flow rate smaller than 1 lt. /min. On the other hand the spray shape was different at different flow rates as shown in Figure 11. At $\Delta P=1.5$ bars. the spray was at the tulip stage with a smooth film and the atomization was coarse. As the pressure drop across the atomizer increased the atomization became finer.

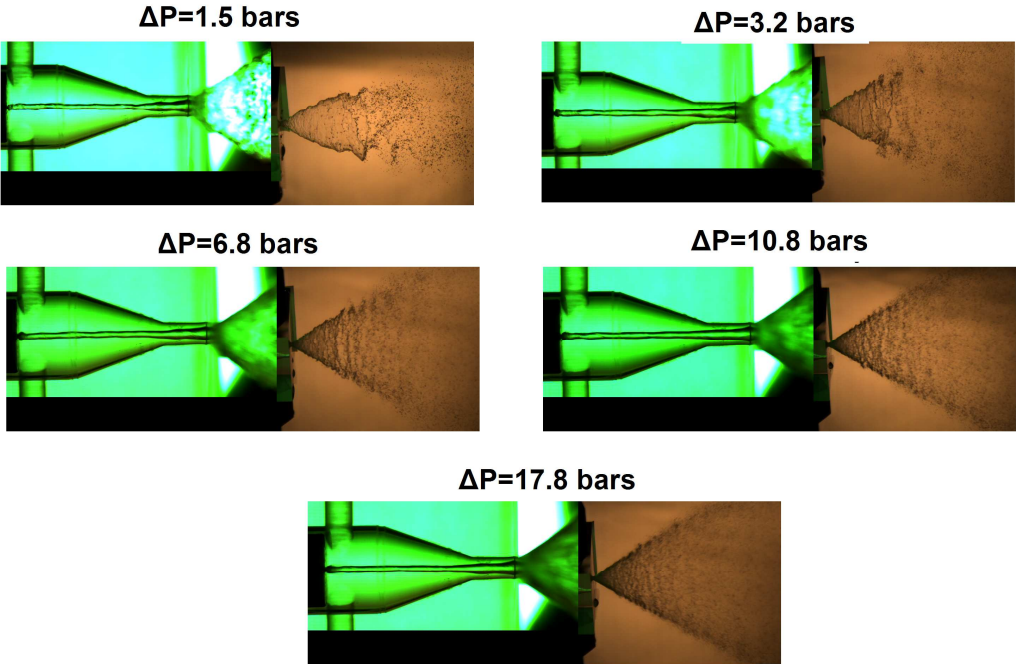


Figure 11: Aircore and the spray for different pressure drops.

Aircore Diameter

The quantitative values of the aircore diameter were obtained using the developed image processing tool, details of which was given in [Sumer2012]. In the present study the mean aircore diameter is evaluated at the mid nozzle for different operating conditions. The variation of mean aircore diameter at mid nozzle with pressure drop is given in Figure12. The air core diameter makes an asymptote at about 1.16 mm as the pressure drop across the atomizer increases.

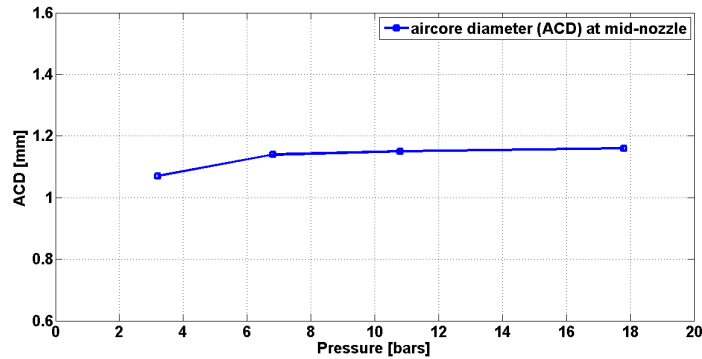


Figure 12: Variation of aircore diameter with pressure drop.

Microscopic Spray Properties

The microscopic properties of the spray measured at 10 different axial locations for different pressure drop values with a two-component phase Doppler particle analyzer (PDPA; TSI Inc.). The origin of the coordinate frame was at the center of the atomizer exit. At each axial location the radial locations (at 3mm intervals) were also traversed and spray properties are measured at about 110 different measurement locations for each case. The properties of different size classes were investigated based on the performed measurements.

The mean velocity vectors for $\Delta P=6.8$ bars (3.18 lt. /min) case are plotted in Figure 13 for two different size classes.

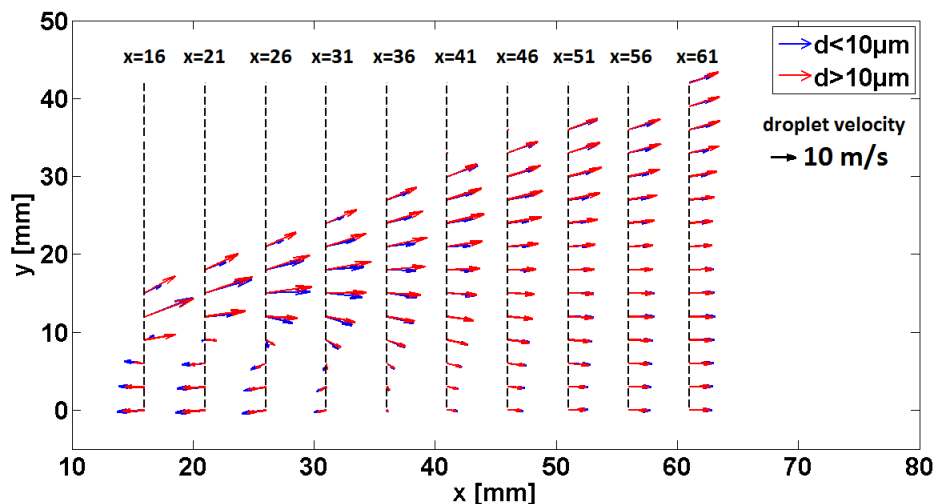


Figure 13: Mean velocity vector plot for different size classes at $\Delta P=6.8$ bar.

At any axial location as one moved from the $y=0$ line (atomizer axis) to higher transverse locations the measured velocity increased, which is typical for hollow cone sprays. A recirculation zone between $x=16$ mm – $x=36$ mm near the atomizer axis was identified and there was a net flow of small droplets into the atomizer at this region.

The mean velocity vectors for $\Delta P=10.8$ bars (4.00 lt. /min) and $\Delta P=17.8$ bars (5.00 lt. /min) are plotted in Figure 14 and Figure 15, respectively, for two different size classes. The main flow characteristics

for $\Delta P=6.8$ bars (3.18 lt. /min) case were also valid for these cases but the recirculation region near the atomizer axis moved towards the atomizer exit as the mass flow rate increased.

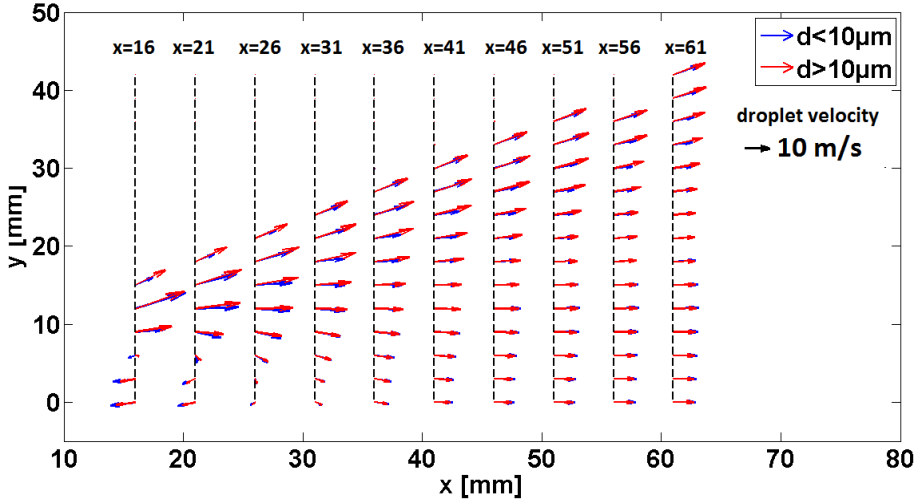


Figure 14: Mean velocity vector plot for different size classes at $\Delta P=10.8$ bar.

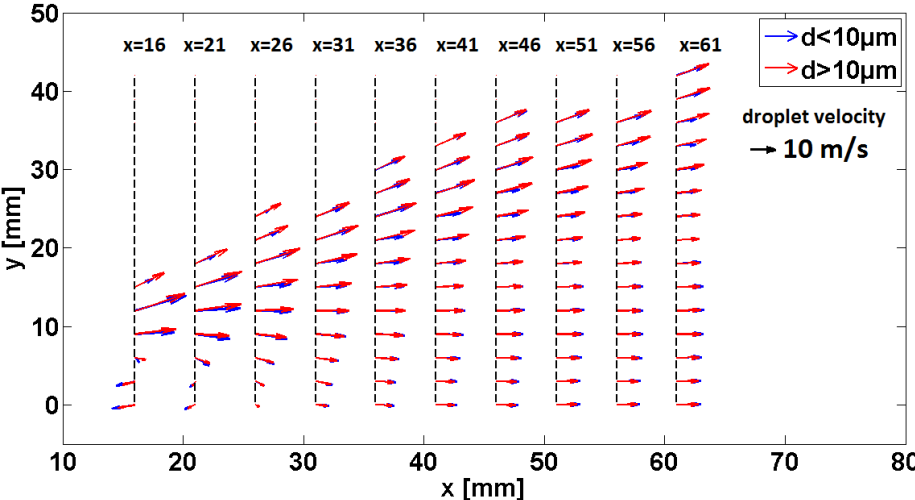


Figure 15: Mean velocity vector plot for different size classes at $\Delta P=17.8$ bar.

The Sauter mean diameter (SMD) distributions at different axial locations are given in Figure 16. In general the SMD decreased as the pressure drop across the atomizer increased.

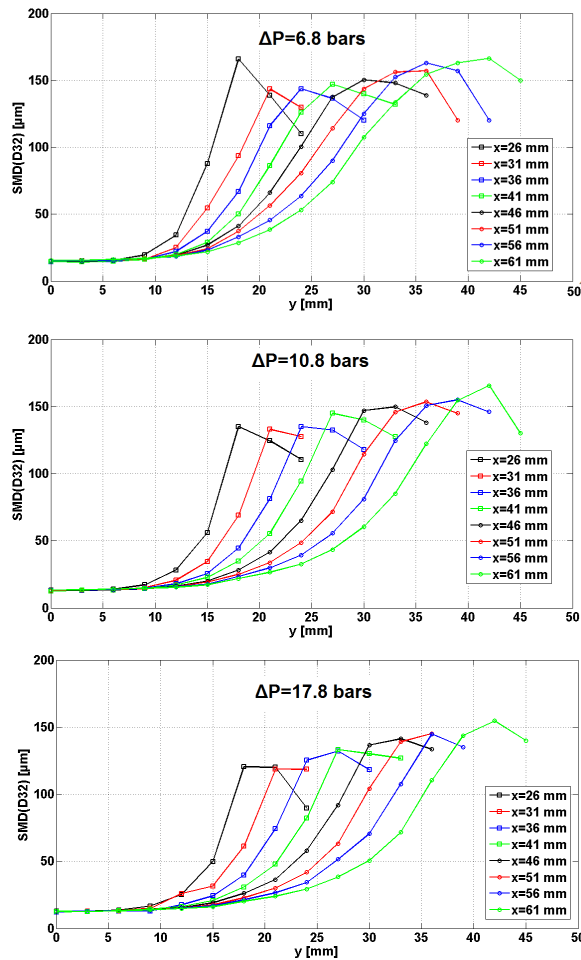


Figure 16: SMD distribution at different axial locations.

Summary and Conclusions

In this study the flow fields inside a pressure swirl atomizer and the resulting hollow cone spray are studied using experimental methods. The formation of the aircore inside the atomizer is explained based on observations. The aircore diameters at mid-nozzle are calculated for different operating conditions. In addition the mean velocity vectors for two different size classes and SMD distributions are plotted at each operating condition.

The main conclusions out of the present study can be listed as follows;

- For the studied atomizer geometry the aircore formation is rather instantaneous and it occurred at mass flow rates below 1 lt./min
- Although at $\Delta P=1.5$ bars (1.0 lt. /min), an aircore present inside the atomizer the resulting spray was at the tulip stage with a smooth film and the atomization was coarse.
- As the mass flow rate through the atomizer increases the film thickness at the mid-nozzle showed an asymptotic behavior.
- Increasing the mass flow rate to 3.18 lt/min results in a fine spray and a typical SMD measure on the spray was about 150 μm at the axial locations of interest.
- A recirculation zone was identified on the spray close to the atomizer exit and it was seen that there is a net flow of small droplets into the atomizer. As the mass flow rate across the atomizer increases the recirculation zone tended to move towards the atomizer exit.

Acknowledgements

This study has been supported by TÜBİTAK-SAGE under Project IBTA founded by State Planning Organization of Turkey. The authors thank Dr. Onur Tuncer for his technical assistance in procurement of the phase Doppler particle analyzer.

References

- Abramovich G.N., The Theory of Swirl Atomizer, Industrial Aerodynamics, BNT ZAGI, Moscow, pp. 114-121, 1944.
- Bachalo W.D. and Houser M.J., Development of the phase Doppler spray analyzer for liquid drop size and velocity characterization. In AIAA/SAE/ASME 20th Joint Propulsion Conference, Cincinnati, Ohio, Bavyel L., Orzechowski Z., Liquid Atomization, Taylor & Francis, Washington, DC, 1984.
- Fu Qing-fei, Yang Li-jun, and Qu Yuan-yuan. , Measurement of annular liquid film thickness in an open-end swirl injector. , *Aerospace Science and Technology*, 15(2):117–124, March 2011.
- Bhardwaj S., and Mittal A., A Survey on Various Edge Detector Techniques, *Procedia Technology*, 4:220–226, 2012.
- Dash S. K., Halder M. R., Peric M., and Som S. K., Formation of Air Core in Nozzles With Tangential Entry. *Journal of Fluids Engineering*, 123(4):829, 2001.
- Durst F. and Zare M., Laser Doppler measurements in two-phase flows., In Proc of the LDA Symposium, pages 403–429, Copenhagen, Denmark, 1975.
- Giffen E., Muraszew A., Atomization of Liquid Fuels, Chapman and Hall, London, 1953.
- Kim Sunghyuk, Khil Taeock, Kim Dongjun, and Yoon Youngbin. , Effect of geometric parameters on the liquid film thickness and air core formation in a swirl injector., *Measurement Science and Technology*, 20(1):015403, January 2009.
- Moon S., Abo-Serie E., and Bae C., Liquid film thickness inside the high pressure swirl injectors: Real scale measurement and evaluation of analytical equations. *Experimental Thermal and Fluid Science*, 34(2):113–121, February 2010.
- Som S.K., Theoretical and Experimental Investigations on the Formation of Air Core in a Spray Atomizing Nozzle. *Applied Scientific Research*, 36:173–196, 1980.
- Som S.K., Theoretical and Experimental Studies on the Formation of an Air Core in a Swirl Spray Pressure Nozzle Using a Power Law Non-Newtonian Liquid. *Applied Scientific Research*, 40:71–91, 1983.
- Som S.K. and Biswas G.W., Initiation of Air Core in a Swirl Nozzle Using Time-Independent Power-Law Fluids. *Acta Mechanica*, 51:179–197, 1984.
- Sumer B., Erkan N., Uzol O., Tuncer İ.H., “Experimental and Numerical Investigation of a Pressure Swirl Atomizer”, ICLASS 2012, 12th Triennial International Conference on Liquid Atomization and Spray Systems, Heidelberg, Germany, September 2-6, 2012.
- Suyari M., and Lefebvre A.H., Film thickness measurements in a simplex swirl atomizer., *Journal of Propulsion and Power*, 2(6):528–533, 1986.
- Taylor G.I., The Mechanics of Swirl Atomizers, vol.2 pt. 1, International Congress of Applied Mechanics, London. 1948.